Tulips R
University of Tsukuba Library

Scleral birefringence as measured by polarization-sensitive optical coherence tomography and ocular biometric parameters of human eyes in vivo

著者	Yamanari Masahiro, Nagase Satoko, Fukuda Shinichi, Ishii Kotaro, Tanaka Ryosuke, Yasui Takeshi, Oshika Tetsuro, Miura Masahiro, Yasuno Yoshiaki
journal or publication title	Biomedical Optics Express
volume	5
number	5
page range	1391-1402
year	2014-05
権利	(C)2014 Optical Society of America. This paper was published in Biomedical Optics Express and is made available as an electronic reprint with the permission of OSA. The paper can be found at the following URL on the OSA website:http://www.opticsinfobase.org/boe/abstract.cfm?uri=boe-5-5-1391. Systematic or multiple reproduction or distribution to multiple locations via electronic or other means is prohibited and is subject to penalties under law.
URL	http://hdl.handle.net/2241/00121634

doi: 10.1364/BOE.5.001391

Biomedical Optics EXPRESS

Scleral birefringence as measured by polarization-sensitive optical coherence tomography and ocular biometric parameters of human eyes *in vivo*

Masahiro Yamanari,[1,4,7] Satoko Nagase,[2,4] Shinichi Fukuda,[3,4] Kotaro Ishii,[3,4] Ryosuke Tanaka,[5] Takeshi Yasui,[5,6] Tetsuro Oshika,[3,4] Masahiro Miura,[2,4] and Yoshiaki Yasuno[1,4,*]

[1]*Computational Optics Group, University of Tsukuba, Tsukuba, Ibaraki, Japan*
[2]*Department of Ophthalmology, Tokyo Medical University Ibaraki Medical Center, Ami, Ibaraki, Japan*
[3]*Department of Ophthalmology, Faculty of Medicine, University of Tsukuba, Tsukuba, Ibaraki, Japan*
[4]*Computational Optics and Ophthalmology Group, Tsukuba, Ibaraki, Japan*
[5]*Graduate School of Engineering Science, Osaka University, Toyonaka, Osaka, Japan*
[6]*Institute of Technology and Science, The University of Tokushima, Tokushima, Tokushima, Japan*
[7]*Tomey Corporation, Nagoya, Aichi, Japan*
[*]*yasuno@optlab2.bk.tsukuba.ac.jp*

Abstract: The relationship between scleral birefringence and biometric parameters of human eyes *in vivo* is investigated. Scleral birefringence near the limbus of 21 healthy human eyes was measured using polarization-sensitive optical coherence tomography. Spherical equivalent refractive error, axial eye length, and intraocular pressure (IOP) were measured in all subjects. IOP and scleral birefringence of human eyes *in vivo* was found to have statistically significant correlations ($r = -0.63$, $P = 0.002$). The slope of linear regression was -2.4×10^{-2} deg/μm/mmHg. Neither spherical equivalent refractive error nor axial eye length had significant correlations with scleral birefringence. To evaluate the direct influence of IOP to scleral birefringence, scleral birefringence of 16 *ex vivo* porcine eyes was measured under controlled IOP of 5–60 mmHg. In these *ex vivo* porcine eyes, the mean linear regression slope between controlled IOP and scleral birefringence was -9.9×10^{-4} deg/μm/mmHg. In addition, porcine scleral collagen fibers were observed with second-harmonic-generation (SHG) microscopy. SHG images of porcine sclera, measured on the external surface at the superior side to the cornea, showed highly aligned collagen fibers parallel to the limbus. In conclusion, scleral birefringence of healthy human eyes was correlated with IOP, indicating that the ultrastructure of scleral collagen was correlated with IOP. It remains to show whether scleral collagen ultrastructure of human eyes is affected by IOP as a long-term effect.

©2014 Optical Society of America

OCIS codes: (170.4500) Optical coherence tomography; (170.4470) Ophthalmology; (050.2555) Form birefringence; (180.4315) Nonlinear microscopy.

References and links

1. N. A. McBrien and A. Gentle, "Role of the sclera in the development and pathological complications of myopia," Prog. Retin. Eye Res. **22**(3), 307–338 (2003).
2. C. F. Burgoyne, J. C. Downs, A. J. Bellezza, J. K. Suh, and R. T. Hart, "The optic nerve head as a biomechanical structure: a new paradigm for understanding the role of IOP-related stress and strain in the pathophysiology of glaucomatous optic nerve head damage," Prog. Retin. Eye Res. **24**(1), 39–73 (2005).
3. J. A. Rada, S. Shelton, and T. T. Norton, "The sclera and myopia," Exp. Eye Res. **82**(2), 185–200 (2006).
4. J. T. Siegwart, Jr. and T. T. Norton, "Regulation of the mechanical properties of tree shrew sclera by the visual environment," Vision Res. **39**(2), 387–407 (1999).

#204494 - $15.00 USD Received 13 Jan 2014; revised 26 Mar 2014; accepted 31 Mar 2014; published 3 Apr 2014

5. N. A. McBrien, L. M. Cornell, and A. Gentle, "Structural and ultrastructural changes to the sclera in a mammalian model of high myopia," Invest. Ophthalmol. Vis. Sci. **42**(10), 2179–2187 (2001).
6. J. K. Pijanka, B. Coudrillier, K. Ziegler, T. Sorensen, K. M. Meek, T. D. Nguyen, H. A. Quigley, and C. Boote, "Quantitative mapping of collagen fiber orientation in non-glaucoma and glaucoma posterior human sclerae," Invest. Ophthalmol. Vis. Sci. **53**(9), 5258–5270 (2012).
7. J. C. Downs, J.-K. F. Suh, K. A. Thomas, A. J. Bellezza, R. T. Hart, and C. F. Burgoyne, "Viscoelastic material properties of the peripapillary sclera in normal and early-glaucoma monkey eyes," Invest. Ophthalmol. Vis. Sci. **46**(2), 540–546 (2005).
8. B. Coudrillier, J. Tian, S. Alexander, K. M. Myers, H. A. Quigley, and T. D. Nguyen, "Biomechanics of the human posterior sclera: Age- and glaucoma-related changes measured using inflation testing," Invest. Ophthalmol. Vis. Sci. **53**(4), 1714–1728 (2012).
9. A. J. Bellezza, C. J. Rintalan, H. W. Thompson, J. C. Downs, R. T. Hart, and C. F. Burgoyne, "Deformation of the lamina cribrosa and anterior scleral canal wall in early experimental glaucoma," Invest. Ophthalmol. Vis. Sci. **44**(2), 623–637 (2003).
10. H. Yang, H. Thompson, M. D. Roberts, I. A. Sigal, J. C. Downs, and C. F. Burgoyne, "Deformation of the early glaucomatous monkey optic nerve head connective tissue after acute IOP elevation in 3-D histomorphometric reconstructions," Invest. Ophthalmol. Vis. Sci. **52**(1), 345–363 (2011).
11. H. A. Quigley, M. E. Dorman-Pease, and A. E. Brown, "Quantitative study of collagen and elastin of the optic nerve head and sclera in human and experimental monkey glaucoma," Curr. Eye Res. **10**(9), 877–888 (1991).
12. S. Nagase, M. Yamanari, R. Tanaka, T. Yasui, M. Miura, T. Iwasaki, H. Goto, and Y. Yasuno, "Anisotropic alteration of scleral birefringence to uniaxial mechanical strain," PLoS ONE **8**(3), e58716 (2013).
13. M. Yamanari, K. Ishii, S. Fukuda, Y. Lim, L. Duan, S. Makita, M. Miura, T. Oshika, and Y. Yasuno, "Optical rheology of porcine sclera by birefringence imaging," PLoS ONE **7**(9), e44026 (2012).
14. R. Oldenbourg, E. D. Salmon, and P. T. Tran, "Birefringence of single and bundled microtubules," Biophys. J. **74**(1), 645–654 (1998).
15. S. K. Nadkarni, M. C. Pierce, B. H. Park, J. F. de Boer, P. Whittaker, B. E. Bouma, J. E. Bressner, E. Halpern, S. L. Houser, and G. J. Tearney, "Measurement of collagen and smooth muscle cell content in atherosclerotic plaques using polarization-sensitive optical coherence tomography," J. Am. Coll. Cardiol. **49**(13), 1474–1481 (2007).
16. C. J. Doillon, M. G. Dunn, E. Bender, and F. H. Silver, "Collagen fiber formation in repair tissue: development of strength and toughness," Coll. Relat. Res. **5**(6), 481–492 (1985).
17. D. A. Parry, "The molecular and fibrillar structure of collagen and its relationship to the mechanical properties of connective tissue," Biophys. Chem. **29**(1-2), 195–209 (1988).
18. G. D. Pins, D. L. Christiansen, R. Patel, and F. H. Silver, "Self-assembly of collagen fibers. influence of fibrillar alignment and decorin on mechanical properties," Biophys. J. **73**(4), 2164–2172 (1997).
19. E. Götzinger, M. Pircher, M. Sticker, A. F. Fercher, and C. K. Hitzenberger, "Measurement and imaging of birefringent properties of the human cornea with phase-resolved, polarization-sensitive optical coherence tomography," J. Biomed. Opt. **9**(1), 94–102 (2004).
20. Y. Yasuno, M. Yamanari, K. Kawana, M. Miura, S. Fukuda, S. Makita, S. Sakai, and T. Oshika, "Visibility of trabecular meshwork by standard and polarization-sensitive optical coherence tomography," J. Biomed. Opt. **15**(6), 061705 (2010).
21. M. G. Ducros, J. D. Marsack, H. G. Rylander III, S. L. Thomsen, and T. E. Milner, "Primate retina imaging with polarization-sensitive optical coherence tomography," J. Opt. Soc. Am. A **18**(12), 2945–2956 (2001).
22. B. Cense, T. C. Chen, B. H. Park, M. C. Pierce, and J. F. de Boer, "Thickness and birefringence of healthy retinal nerve fiber layer tissue measured with polarization-sensitive optical coherence tomography," Invest. Ophthalmol. Vis. Sci. **45**(8), 2606–2612 (2004).
23. M. Yamanari, M. Miura, S. Makita, T. Yatagai, and Y. Yasuno, "Phase retardation measurement of retinal nerve fiber layer by polarization-sensitive spectral-domain optical coherence tomography and scanning laser polarimetry," J. Biomed. Opt. **13**(1), 014013 (2008).
24. M. Miura, M. Yamanari, T. Iwasaki, A. E. Elsner, S. Makita, T. Yatagai, and Y. Yasuno, "Imaging polarimetry in age-related macular degeneration," Invest. Ophthalmol. Vis. Sci. **49**(6), 2661–2667 (2008).
25. Y. Yasuno, M. Yamanari, K. Kawana, T. Oshika, and M. Miura, "Investigation of post-glaucoma-surgery structures by three-dimensional and polarization sensitive anterior eye segment optical coherence tomography," Opt. Express **17**(5), 3980–3996 (2009).
26. Y. Lim, M. Yamanari, S. Fukuda, Y. Kaji, T. Kiuchi, M. Miura, T. Oshika, and Y. Yasuno, "Birefringence measurement of cornea and anterior segment by office-based polarization-sensitive optical coherence tomography," Biomed. Opt. Express **2**(8), 2392–2402 (2011).
27. M. Yamanari, S. Makita, and Y. Yasuno, "Polarization-sensitive swept-source optical coherence tomography with continuous source polarization modulation," Opt. Express **16**(8), 5892–5906 (2008).
28. M. Yamanari, Y. Lim, S. Makita, and Y. Yasuno, "Visualization of phase retardation of deep posterior eye by polarization-sensitive swept-source optical coherence tomography with 1- μm probe," Opt. Express **17**(15), 12385–12396 (2009).
29. M. Yamanari, S. Makita, Y. Lim, and Y. Yasuno, "Full-range polarization-sensitive swept-source optical coherence tomography by simultaneous transversal and spectral modulation," Opt. Express **18**(13), 13964–13980 (2010).
30. M. Miura, M. Yamanari, T. Iwasaki, M. Itoh, T. Yatagai, and Y. Yasuno, "Polarization-sensitive optical coherence tomography of necrotizing scleritis," Ophthalmic Surg. Lasers Imaging **40**(6), 607–610 (2009).

#204494 - $15.00 USD Received 13 Jan 2014; revised 26 Mar 2014; accepted 31 Mar 2014; published 3 Apr 2014
(C) 2014 OSA

31. S. Makita, M. Yamanari, and Y. Yasuno, "Generalized jones matrix optical coherence tomography: performance and local birefringence imaging," Opt. Express **18**(2), 854–876 (2010).
32. L. Duan, S. Makita, M. Yamanari, Y. Lim, and Y. Yasuno, "Monte-carlo-based phase retardation estimator for polarization sensitive optical coherence tomography," Opt. Express **19**(17), 16330–16345 (2011).
33. A. Alm and S. F. Nilsson, "Uveoscleral outflow--a review," Exp. Eye Res. **88**(4), 760–768 (2009).
34. S. Sakai, M. Yamanari, Y. Lim, N. Nakagawa, and Y. Yasuno, "*In vivo* evaluation of human skin anisotropy by polarization-sensitive optical coherence tomography," Biomed. Opt. Express **2**(9), 2623–2631 (2011).
35. T. W. Olsen, S. Sanderson, X. Feng, and W. C. Hubbard, "Porcine sclera: Thickness and surface area," Invest. Ophthalmol. Vis. Sci. **43**(8), 2529–2532 (2002).
36. B. K. Pierscionek, M. Asejczyk-Widlicka, and R. A. Schachar, "The effect of changing intraocular pressure on the corneal and scleral curvatures in the fresh porcine eye," Br. J. Ophthalmol. **91**(6), 801–803 (2007).
37. D. S. Schultz, J. C. Lotz, S. M. Lee, M. L. Trinidad, and J. M. Stewart, "Structural factors that mediate scleral stiffness," Invest. Ophthalmol. Vis. Sci. **49**(10), 4232–4236 (2008).
38. S. Nicoli, G. Ferrari, M. Quarta, C. Macaluso, P. Govoni, D. Dallatana, and P. Santi, "Porcine sclera as a model of human sclera for in vitro transport experiments: histology, sem, and comparative permeability," Mol. Vis. **15**, 259–266 (2009).
39. M. J. A. Girard, J.-K. F. Suh, M. Bottlang, C. F. Burgoyne, and J. C. Downs, "Biomechanical changes in the sclera of monkey eyes exposed to chronic iop elevations," Invest. Ophthalmol. Vis. Sci. **52**(8), 5656–5669 (2011).
40. P. M. Pinsky, D. van der Heide, and D. Chernyak, "Computational modeling of mechanical anisotropy in the cornea and sclera," J. Cataract Refract. Surg. **31**(1), 136–145 (2005).
41. R. Grytz and G. Meschke, "A computational remodeling approach to predict the physiological architecture of the collagen fibril network in corneo-scleral shells," Biomech. Model. Mechanobiol. **9**(2), 225–235 (2010).
42. Collaborative Normal-Tension Glaucoma Study Group, "Comparison of glaucomatous progression between untreated patients with normal-tension glaucoma and patients with therapeutically reduced intraocular pressures," Am. J. Ophthalmol. **126**(4), 487–497 (1998).
43. Y. Suzuki, A. Iwase, M. Araie, T. Yamamoto, H. Abe, S. Shirato, Y. Kuwayama, H. K. Mishima, H. Shimizu, G. Tomita, Y. Inoue, and Y. Kitazawa; Tajimi Study Group, "Risk factors for open-angle glaucoma in a japanese population: The tajimi study," Ophthalmology **113**(9), 1613–1617 (2006).
44. M. J. A. Girard, J. C. Downs, C. F. Burgoyne, and J.-K. F. Suh, "Peripapillary and posterior scleral mechanics--part i: Development of an anisotropic hyperelastic constitutive model," J. Biomech. Eng. **131**(5), 051011 (2009).
45. B. Coudrillier, C. Boote, H. A. Quigley, and T. D. Nguyen, "Scleral anisotropy and its effects on the mechanical response of the optic nerve head," Biomech. Model. Mechanobiol. **12**(5), 941–963 (2013).
46. M. J. Hogan, J. A. Alvarado, and J. E. Weddell, *Histology of the human eye: an atlas and textbook* (Saunders, 1971).
47. H. A. Quigley, E. M. Addicks, W. R. Green, and A. E. Maumenee, "Optic nerve damage in human glaucoma. Ii. the site of injury and susceptibility to damage," Arch. Ophthalmol. **99**(4), 635–649 (1981).
48. Y. Lim, Y.-J. Hong, L. Duan, M. Yamanari, and Y. Yasuno, "Passive component based multifunctional jones matrix swept source optical coherence tomography for doppler and polarization imaging," Opt. Lett. **37**(11), 1958–1960 (2012).
49. T. Torzicky, S. Marschall, M. Pircher, B. Baumann, M. Bonesi, S. Zotter, E. Götzinger, W. Trasischker, T. Klein, W. Wieser, B. Biedermann, R. Huber, P. Andersen, and C. K. Hitzenberger, "Retinal polarization-sensitive optical coherence tomography at 1060 nm with 350 khz a-scan rate using an fourier domain mode locked laser," J. Biomed. Opt. **18**(2), 026008 (2013).
50. M. C. van Turnhout, S. Kranenbarg, and J. L. van Leeuwen, "Modeling optical behavior of birefringent biological tissues for evaluation of quantitative polarized light microscopy," J. Biomed. Opt. **14**(5), 054018 (2009).
51. P. Watson and B. Hazleman, *The Sclera and Systemic Disorders* (Jp Medical Pub, 2012).
52. R. H. Newton and K. M. Meek, "The integration of the corneal and limbal fibrils in the human eye," Biophys. J. **75**(5), 2508–2512 (1998).
53. D. Yan, S. McPheeters, G. Johnson, U. Utzinger, and J. P. Vande Geest, "Microstructural differences in the human posterior sclera as a function of age and race," Invest. Ophthalmol. Vis. Sci. **52**(2), 821–829 (2011).
54. M. J. A. Girard, A. Dahlmann-Noor, S. Rayapureddi, J. A. Bechara, B. M. E. Bertin, H. Jones, J. Albon, P. T. Khaw, and C. R. Ethier, "Quantitative mapping of scleral fiber orientation in normal rat eyes," Invest. Ophthalmol. Vis. Sci. **52**(13), 9684–9693 (2011).
55. N. Morishige, A. J. Wahlert, M. C. Kenney, D. J. Brown, K. Kawamoto, T.-i. Chikama, T. Nishida, and J. V. Jester, "Second-harmonic imaging microscopy of normal human and keratoconus cornea," Invest. Ophthalmol. Vis. Sci. **48**(3), 1087–1094 (2007).
56. J. M. Bueno, E. J. Gualda, A. Giakoumaki, P. Pérez-Merino, S. Marcos, and P. Artal, "Multiphoton microscopy of ex vivo corneas after collagen cross-linking," Invest. Ophthalmol. Vis. Sci. **52**(8), 5325–5331 (2011).
57. N. Morishige, N. Yamada, X. Zhang, Y. Morita, N. Yamada, K. Kimura, A. Takahara, and K.-H. Sonoda, "Abnormalities of stromal structure in the bullous keratopathy cornea identified by second harmonic generation imaging microscopy," Invest. Ophthalmol. Vis. Sci. **53**(8), 4998–5003 (2012).
58. M. Han, G. Giese, and J. Bille, "Second harmonic generation imaging of collagen fibrils in cornea and sclera," Opt. Express **13**(15), 5791–5797 (2005).
59. S.-W. Teng, H.-Y. Tan, J.-L. Peng, H.-H. Lin, K. H. Kim, W. Lo, Y. Sun, W.-C. Lin, S.-J. Lin, S.-H. Jee, P. T. C. So, and C.-Y. Dong, "Multiphoton autofluorescence and second-harmonic generation imaging of the ex vivo porcine eye," Invest. Ophthalmol. Vis. Sci. **47**(3), 1216–1224 (2006).

#204494 - $15.00 USD Received 13 Jan 2014; revised 26 Mar 2014; accepted 31 Mar 2014; published 3 Apr 2014
(C) 2014 OSA

60. A. Miyazawa, M. Yamanari, S. Makita, M. Miura, K. Kawana, K. Iwaya, H. Goto, and Y. Yasuno, "Tissue discrimination in anterior eye using three optical parameters obtained by polarization sensitive optical coherence tomography," Opt. Express **17**(20), 17426–17440 (2009).
61. L. Duan, M. Yamanari, and Y. Yasuno, "Automated phase retardation oriented segmentation of chorio-scleral interface by polarization sensitive optical coherence tomography," Opt. Express **20**(3), 3353–3366 (2012).
62. T. Torzicky, M. Pircher, S. Zotter, M. Bonesi, E. Götzinger, and C. K. Hitzenberger, "Automated measurement of choroidal thickness in the human eye by polarization sensitive optical coherence tomography," Opt. Express **20**(7), 7564–7574 (2012).
63. J. Liu and C. J. Roberts, "Influence of corneal biomechanical properties on intraocular pressure measurement," J. Cataract Refract. Surg. **31**(1), 146–155 (2005).

1. Introduction

Recent studies have suggested that the biomechanical property of sclera of myopic and glaucomatous eyes is different from that of normal eyes [1–3]. Sclera of the myopic eye is known to have increased creep [4], decreased thickness, and smaller collagen fibril diameter [1,5]. These changes are believed to be associated with the remodeling of the sclera and the axial elongation of the eyeball. Although the alignment of scleral collagen fibers in glaucomatous eyes is not known well, Pijanka et al. reported that sclerae of some glaucomatous eyes had decreased fiber anisotropy of collagen fibers in two quadrant sectors around the optic nerve head [6]. The stiffness of the peripapillary sclera of glaucomatous eyes was different from that of normal eyes in the cases of experimental monkeys and postmortem humans [7–10]. Glaucomatous human eyes had lower density of collagen fibers in peripapillary sclera than that of normal human eyes [11].

Although the scleral biomechanics has important roles for myopia and glaucoma, *in vivo* scleral biomechanics has been poorly investigated. Recently, we showed that the elasticity of *ex vivo* porcine sclera correlated with the birefringence that was measured by polarization-sensitive optical coherence tomography (PS-OCT) [12,13]. The result can be understood from two known facts that highly organized collagen fiber has high birefringence [14,15] and that highly organized collagen fiber has high elasticity [1,16–18].

PS-OCT, which is a functional extension of OCT, can measure birefringence of sclera and many other ocular tissues noninvasively without contact. PS-OCT has been used to measure birefringence of cornea [19], trabecular meshwork [20], retinal nerve fibers [21–23], and scarred tissue of age-related macular degeneration [24]. PS-OCT has also been used to investigate birefringence of pterygium and scarred tissue of the conjunctiva after trabeculectomy [25,26]. Although it is known that the sclera has high birefringence in both the anterior and posterior segments of the eye [27–29], the association of scleral birefringence with ocular diseases has not been investigated to date except in one case study of necrotizing scleritis [30]. The birefringence properties of healthy sclera are likewise not well known.

In this paper, we show the relationships between birefringence of *in vivo* human sclera and biometric parameters of the human eye. In addition, we show that the birefringence of sclera is not significantly influenced by short-term alteration of intraocular pressure (IOP) in the case of *ex vivo* porcine eyes. Regionally different fiber structures of the *ex vivo* porcine sclera are also visualized using second-harmonic-generation (SHG) microscopy.

2. Methods

2.1 Measurement of in vivo human sclera

Twenty-one left eyes of healthy human subjects without marked disorders were involved in this study. The protocol adhered to the tenets of the Declaration of Helsinki and was approved by the Institutional Review Board at the University of Tsukuba. Informed consent was obtained from each participant after explanation of the study.

Axial eye length, spherical equivalent refractive error, and IOP of the healthy human eyes were measured by IOL Master (Carl Zeiss Meditec, Dublin, CA, USA), auto kerato-refractometer (RT-7000, Tomey Corp., Nagoya, Aichi, Japan), and Goldmann applanation tonometer, respectively.

#204494 - $15.00 USD Received 13 Jan 2014; revised 26 Mar 2014; accepted 31 Mar 2014; published 3 Apr 2014
(C) 2014 OSA

Birefringence of the sclera was measured by our prototype of PS-OCT [26]. In brief, the system used a frequency-swept light source with center wavelength and scanning speed of 1.31 μm and 30 kHz, respectively. The axial resolution was 9.2 μm in tissue. Using polarization modulation and polarization-sensitive detection, the system measures a tomography of Jones matrix of a sample, which represents the polarization property of the sample. Using this system, we measured volumetric data in a lateral measurement range of 6 mm × 3 mm on the sample, with 512 × 128 A-scans. Figure 1(a) shows a representative OCT intensity image of human sclera near the limbus. The angle of anterior chamber was included in the right side of the image as a landmark of the measurement.

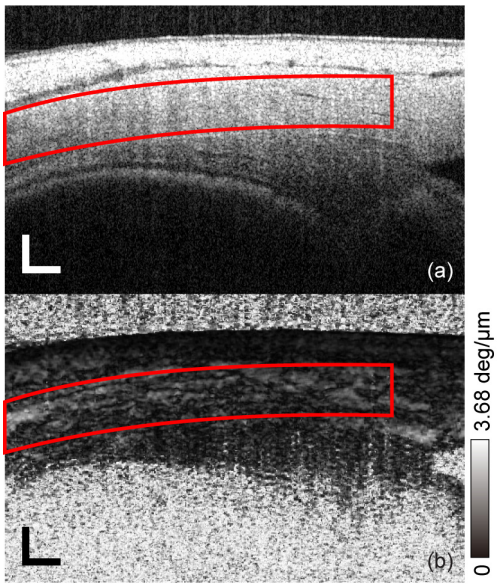

Fig. 1. Representative OCT intensity (a) and local birefringence (b) images of human sclera in vivo. Red outlined areas show the extracted region used to calculate averaged birefringence in each sample. Scale bar represents 500 μm × 500 μm.

To analyze the polarization property of the sclera, we calculated local birefringence from the measured Jones matrix. To calculate the local birefringence of the sclera, we used a similar method developed previously [13]. The Jones matrices were moving-averaged with a kernel size of 3 pix (axial) × 5 pix (transversal) (18 μm × 59 μm) in each B-scan after cancelling the relative global phase among the Jones matrices [26]. Local birefringence of sclera was calculated using the method published previously [31]. The local birefringence was calculated from the depth-oriented alteration of the polarization property in a small depth-region. The size of the region was 8 pix (49 μm) in tissue, which represented the spatial resolution of the measured local birefringence. Figure 1(b) shows the local birefringence image of human sclera. Some domains that have high birefringence are visible in the sclera, which would represent inhomogeneity in collagen fibers.

A scleral region was extracted semi-automatically as indicated by the outlined red areas shown in Fig. 1(a) and 1(b). In addition, the pixels that had lower effective signal to noise ratio than 10 dB or lower degree of optic axis uniformity than 0.9 [13] were excluded from the subsequent analysis. The measured local birefringence value was converted to an estimated birefringence value using a Monte Carlo-based estimator [32]. By averaging the estimated birefringence value in each volume of sclera, a true averaged local birefringence value was obtained [32].

#204494 - $15.00 USD Received 13 Jan 2014; revised 26 Mar 2014; accepted 31 Mar 2014; published 3 Apr 2014
(C) 2014 OSA

2.2 Inflation response of ex vivo porcine sclera

To observe the influence of short-term alteration of IOP on the birefringence of the sclera, we measured the birefringence of porcine sclera with controlled IOP. Sixteen porcine eyes obtained from a local abattoir were used for the experiment within the same day of the sacrifice. Extraocular tissues and conjunctiva were removed before the experiment.

Figure 2 shows the schematic of the experiment designed to measure birefringence of the *ex vivo* porcine sclera in response to the inflation of the eye. IOP was controlled by a reservoir of phosphate-buffered solution (PBS) (BSS Plus, Alcon, Fort Worth, TX, USA). The reservoir was connected to a 24G cannula inserted into the optic nerve head of the porcine eye. IOP was monitored by a pressure sensor (MLT0699, ADInstruments, Bella Vista, NSW, Australia) that was located at the same height as the eye. The height of the liquid level was controlled manually to change the IOP of the eye from 5 to 60 mmHg with eight steps (5, 10, 14, 18, 22, 30, 45, and 60 mmHg).

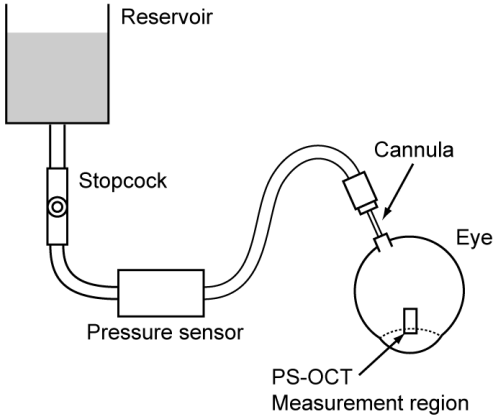

Fig. 2. Schematic of the experiment designed to measure the inflation response of scleral birefringence.

Birefringence of the porcine sclera was measured at each controlled IOP using the PS-OCT. Figure 3 shows representative OCT intensity and local birefringence images. The measured region and the processing method to calculate the birefringence were the same as the experiment using the *in vivo* human sclera.

#204494 - $15.00 USD Received 13 Jan 2014; revised 26 Mar 2014; accepted 31 Mar 2014; published 3 Apr 2014
(C) 2014 OSA

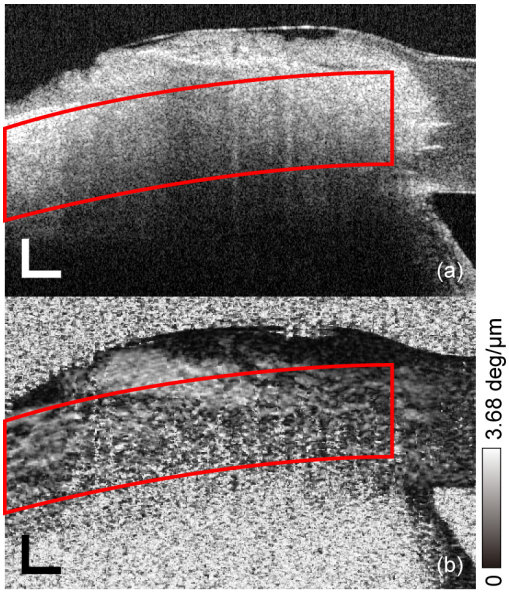

Fig. 3. Representative OCT intensity (a) and local birefringence (b) images of porcine sclera *ex vivo*. Red outlined areas show the extracted region used to calculate averaged birefringence in each sample. Scale bar represents 500 μm × 500 μm.

2.3 SHG imaging of porcine sclera

To observe the structure of collagen fibers in the sclera, we measured backscattering from the sclera with SHG microscopy. The light source was a femtosecond laser (center wavelength, 800 nm; pulse width, ~100 fs; repetition rate, 80 MHz; average output power, ~30 mW). The incident state of polarization was controlled to be circular polarization with a quarter waveplate so that the signal intensity of the SHG did not depend on the orientation of the collagen fiber. The light illuminates the sample from the bottom side through an inverted light microscope (TE2000-U, Nikon, Tokyo, Japan) where the light is focused by an oil-immersion lens (20 × , NA = 1) that contacts a glass slide. The sample was set on the glass slide. Backscattered SHG signal was separated from the fundamental wavelength, and detected by a photomultiplier tube. The gain of the detector was controlled to optimize the image contrast for each image.

Six porcine eyes were dissected for this measurement by SHG microscopy. Two scleral strips with a size of 5 mm square were extracted from each eye at the superior side of the cornea and at the posterior pole that did not include a peripapillary region. The scleral strip extracted at the superior side of the cornea was directly mounted on a glass slide, and measured by SHG microscopy. Both external and internal surfaces of the sclera were measured for each strip. The other scleral strip extracted at the posterior pole was immersed in paraffin, frozen by liquid nitrogen, sectioned in a low temperature cryostat at a thickness of 30 μm, and at a depth of 600 μm from the external surface of the sclera, mounted on a glass slide, and measured by SHG microscopy.

3. Results

Figure 4 shows the plots of birefringence as a function of biometric parameters of spherical equivalent refractive error (a), axial eye length (b), and IOP (c). Statistically significant correlation was found between the birefringence and the IOP (two-sided test using Pearson's correlation coefficient, r = –0.63, P = 0.002). The slope and intercept of the linear regression line were $–2.4 \times 10^{–2}$ deg/μm/mmHg and 1.5 deg/μm, respectively. The results did not show

#204494 - $15.00 USD Received 13 Jan 2014; revised 26 Mar 2014; accepted 31 Mar 2014; published 3 Apr 2014
(C) 2014 OSA

statistically significant correlations between birefringence and spherical equivalent refractive error or axial eye length.

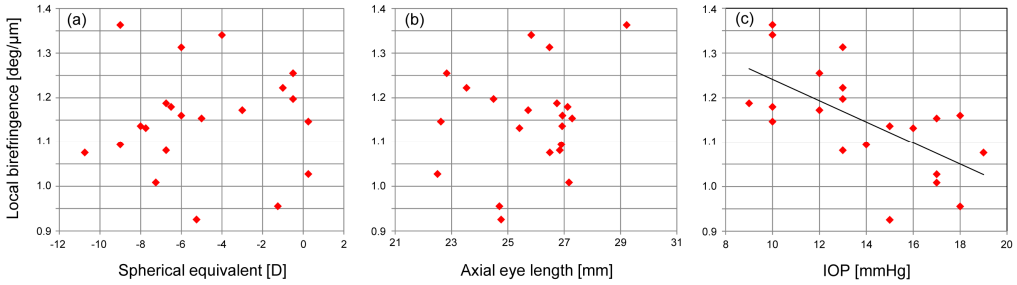

Fig. 4. Plots of local birefringence of the human sclera and spherical equivalent (a), axial eye length (b), and IOP (c).

Figure 5 shows the plots of birefringence at the controlled IOP for each porcine eye. To determine the dependence of birefringence on the IOP, linear regression was applied for each eye. Mean slope was -9.9×10^{-4} deg/μm/mmHg.

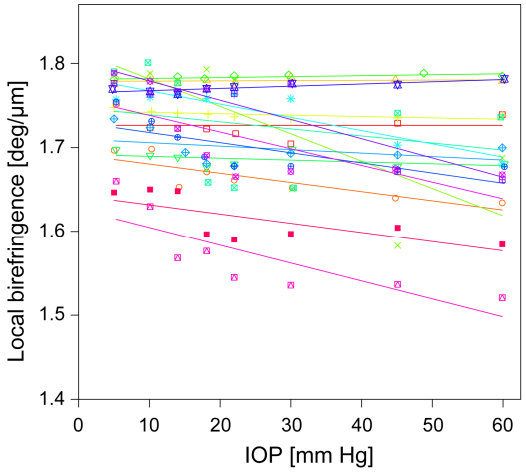

Fig. 5. Plots of local birefringence of the porcine sclera and controlled IOP. Linear regression line of each porcine eye is also shown. Each color represents a different eye.

Figure 6 shows the scatter plot of the slope between the scleral birefringence and IOP of *in vivo* human eyes (black rectangle) and *ex vivo* porcine eyes (white rectangles). The minimum slope of 16 porcine eyes was less than 15% of the average of 21 human eyes without controlled IOP.

#204494 - $15.00 USD Received 13 Jan 2014; revised 26 Mar 2014; accepted 31 Mar 2014; published 3 Apr 2014
(C) 2014 OSA

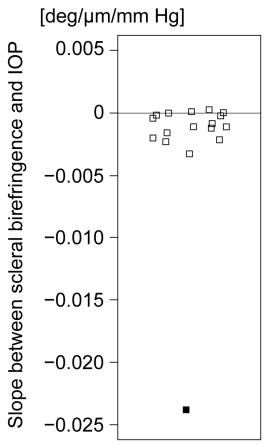

Fig. 6. Scatter plot of the slope between scleral birefringence and IOP. Filled square and open squares show the results of in vivo human eyes and ex vivo porcine eyes, respectively.

Figure 7 shows the SHG images at the superior side of the cornea of porcine eyes *ex vivo*. On the external surface of the sclera (row A of Fig. 7), SHG images showed clear collagen bundles that roughly aligned in the horizontal direction, which were parallel to the limbus. At the depth of 600 μm, as shown in row B of Fig. 7, the contrast of collagen bundles was not as clear as at the external surface. This could be partly because the sliced plane was not parallel to the fiber. On the internal surface of the sclera (row C of Fig. 7), the contrast of collagen fiber was not clear, and the collagen fiber did not have a specific orientation of alignment. Because the detector gain was optimized for each SHG image, the contrasts of all images are nearly the same. However, the raw SHG intensity from the internal surfaces was significantly weaker than at the external surfaces.

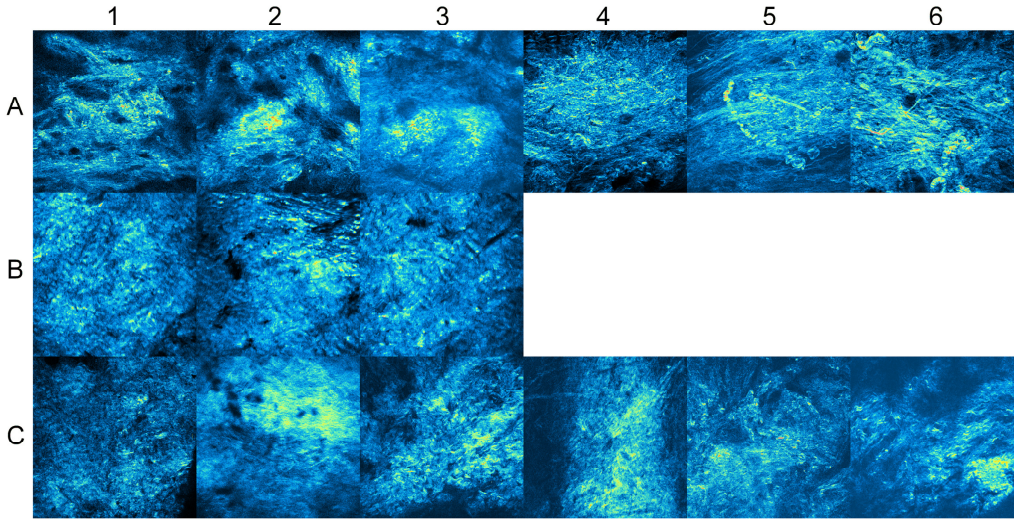

Fig. 7. SHG microscopy images of the porcine sclera at the superior side of the cornea. Rows A, B, and C show the SHG images on the external surface, at the depth of 600 μm, and on the internal surface of the sclera, respectively. The numbers of the columns from 1 to 6 show IDs of porcine eyes.

Figure 8 shows the SHG images of the porcine sclera at the posterior pole. On the external surface (row A of Fig. 8), SHG images clearly showed undulating thick bundles, which had a

#204494 - $15.00 USD Received 13 Jan 2014; revised 26 Mar 2014; accepted 31 Mar 2014; published 3 Apr 2014
(C) 2014 OSA

width of 20–50 μm. The bundles had interwoven structures with various orientations. There was no notable major orientation of the fiber bundles. At the depth of 600 μm (row B of Fig. 8), the contrast of collagen bundles was better than that observed near the limbus, as shown in Fig. 7. On the internal surface of the sclera (row C of Fig. 8), fine collagen bundles were observed in eyes 1 and 2. These bundles had a diameter of 3–5 μm and were frequently branched and intermingled. In the other eyes, the images looked fuzzy, and individual bundles were not as clear as in the other eyes.

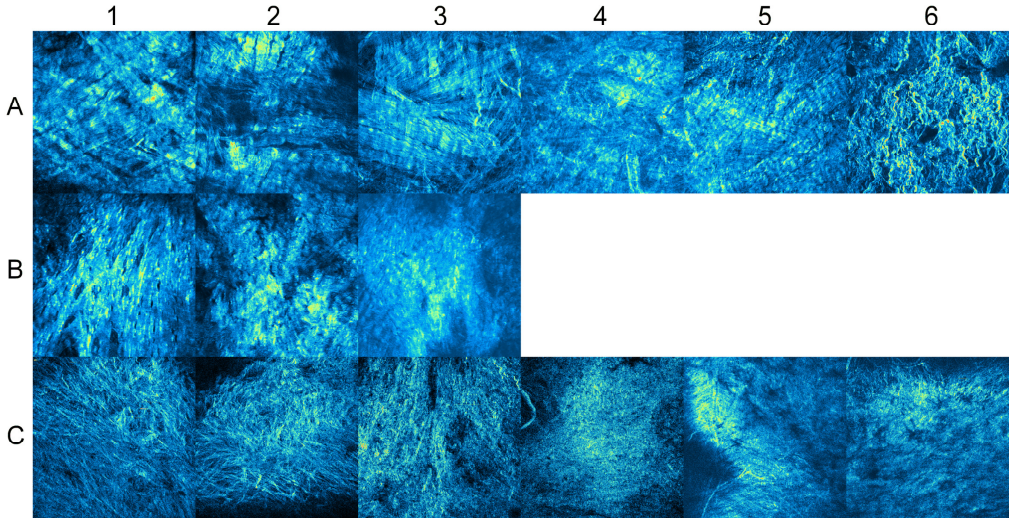

Fig. 8. SHG images of the porcine sclera at the posterior pole. Rows A, B, and C show the SHG images on the external surface, at the depth of 600 μm, and on the internal surface of the sclera, respectively. The numbers of the columns from 1 to 6 show IDs of porcine eyes.

4. Discussion

In the study of *in vivo* human eyes, we investigated the relationship between birefringence and biometric parameters. The IOP showed statistically significant correlation with the birefringence, while the spherical equivalent refractive error and axial eye length did not show these correlations in this small number of subjects. To further explain the relationship between the IOP and birefringence, several mechanisms can be hypothesized.

The first hypothesis is that the ultrastructure of the sclera has a role in regulating IOP. However, the sclera is not the main resistance component for both trabecular and uveoscleral outflow [33], and it is unlikely that scleral ultrastructure affects the IOP directly, at least in the normal eyes.

Another hypothesis is that short-term alteration of IOP could affect the birefringence, because the alteration of IOP may change the density of collagen fibrils or the anisotropy of collagen fibers. For example, it was reported that the birefringence of human skin was altered by stretching [34]. To examine this hypothesis, the birefringence of the porcine sclera was measured under controlled IOP. The results disproved this hypothesis for the porcine sclera. The short-term alteration of IOP did not significantly affect the scleral birefringence in the case of porcine eyes *ex vivo*. Although it has been known that human and porcine eyes have similar properties of the sclera in some aspects [35-38], additional studies would be required to show whether the outcome of porcine eyes is interchangeable to human eyes. If it was exchangeable, our result would suggest that the short-term alteration of IOP does not explain the significant negative relationship between the IOP and scleral birefringence of human eyes *in vivo*. This validation is still left as a future work.

Assuming interchangeability between porcine and human eyes as discussed above and considering the structural source of the birefringent tissues, our results may indicate that

#204494 - $15.00 USD Received 13 Jan 2014; revised 26 Mar 2014; accepted 31 Mar 2014; published 3 Apr 2014
(C) 2014 OSA

because of unknown factors, the sclera of healthy eyes with relatively high IOP had low density collagen fibrils or irregular orientations of the collagen fibers. One possible but not proven hypothesis is that chronic elevation of IOP affects the tissue remodeling process of sclera [39] and the scleral birefringence could have been gradually decreased over time.

Previously, we showed that birefringence and elasticity of sclera were positively correlated [13]. Considering this report and the results of our study, human eyes may have different scleral biomechanical properties depending on their inherent IOP. However, further studies are necessary to validate this hypothesis.

In our other recent paper [12], we reported that the birefringence of porcine sclera was altered by uniaxial strain in both meridional and equatorial directions. However, the alteration of birefringence in the inflation test in the current study was smaller than that with the uniaxial strain. The different results of these studies are likely to be explained by the different protocols of the applied pressure. Since one can assume that the inflation test imposes almost equibiaxial loading condition, only little reorganization of the collagen structure is occurred. This would explain why birefringence was not significantly altered with IOP for the porcine sclera. One additional thought is about strain at limbus. The IOP elevation would not always produce an equibiaxial loading at the limbus because of the abrupt change in curvature between the sclera and the cornea. It would be expected that the birefringence alteration at limbus under IOP alteration is not the same with the scleral region measured in the current study. It is an important future study and is potentially important for the computational models of the sclera, which assume that collagen fibers and matrix deforms according to the macroscopic deformation of the tissue [39–41].

Both IOP and scleral biomechanics are known to have important roles in glaucoma. Lowering IOP is an effective treatment for both normal tension glaucoma [42] and primary open angle glaucoma [43]. It is also known that the scleral biomechanics is likely related to the arrangement of collagen fibers [44,45]. For example, it was reported that some glaucomatous human eyes had lower anisotropy of collagen fibers in the posterior sclera [6]. In addition, it was also reported that glaucomatous human eyes had lower density of collagen fibers in peripapillary sclera [11]. These reports may indicate that the ultrastructure of sclera is related to the progression of glaucoma. Since it is known that the organization of collagen fibers is related to the birefringence [14,15], it would be of interest to investigate scleral birefringence of normal and glaucomatous eyes in future.

Although the posterior sclera has high isotropy of collagen fibers, peripapillary sclera is known to have anisotropic fiber orientation along the circumferential direction of the optic nerve head [6,46]. Although it has not been validated yet, we speculate that the anisotropic fiber of the peripapillary sclera may be related to the high birefringence of peripapillary sclera measured previously by PS-OCT [28,29]. Peripapillary sclera has been extensively investigated, because it is known to play an important role in the deformation of lamina cribrosa [47]. Since the stiffness of the peripapillary sclera of glaucomatous eyes was different from that of normal eyes in the cases of experimental monkeys and postmortem humans [7–10], it is likely that the stiffness of the peripapillary sclera is related to the progression of glaucoma. In the future, it would be interesting to investigate birefringence of peripapillary sclera in normal and glaucomatous eyes using PS-OCT especially designed for posterior segment imaging [28,48,49].

Highly intertwined and interwoven structures of collagen fibers could have decreased total birefringence, because the birefringence of collagen fibers with different orientations partly cancels each other [14,50]. Hence, the birefringence at the posterior region, where the randomness of fiber orientation of sclera is relatively high, would be lower than that of the region near the limbus. Further understanding of the relationship between the birefringence and ultrastructural properties of the sclera would be important to strengthen the use of PS-OCT for evaluating mechanical properties of tissues.

As shown in Fig. 7, SHG microscopy showed that the collagen fiber of sclera was parallel to the limbus. This is consistent with previous reports about the scleral structure [46,51,52]. In contrast, the collagen fiber of the posterior sclera shown in Fig. 8 had various orientations.

#204494 - $15.00 USD Received 13 Jan 2014; revised 26 Mar 2014; accepted 31 Mar 2014; published 3 Apr 2014
(C) 2014 OSA

This is also consistent with previous reports that measured scleral fiber anisotropy with small-angle light scattering (SALS) [53,54]. The unclear SHG image on the internal surface of the sclera (rows C of Figs. 7 and 8) might be due to the smaller diameter of collagen fibrils [5].

Although SHG microscopy has been frequently used for corneal imaging [55–57], there are only a few reports of its application to scleral imaging [58,59]. As shown in Figs. 7 and 8, we demonstrated that SHG microscopy is useful in observing the orientation and anisotropy of collagen fibers that have regional differences in the sclera. Although it is difficult to resolve individual collagen fibrils by SHG microscopy, it has the advantage of observing collagen bundles in a wider field of view than scanning electron microscopy, and of enabling imaging of both stained and unstained samples *in situ*.

There are several limitations in this study. First, we used *ex vivo* porcine eyes in the experiment of inflation response of birefringence, because it is difficult to control the IOP of human eyes *in vivo* noninvasively. A possible *in vivo* human experiment would be measurements before and after intravitreal injection during true clinical treatments. This would be the next study for a more detailed investigation. Second, we only measured healthy eyes within normal IOP ranges in the *in vivo* experiment. Studies with highly myopic eyes and glaucomatous eyes would extend the current understanding about the relationship between birefringence and biometric parameters. Third, we measured birefringence of the sclera only close to the limbus. The birefringence may be different depending on the region, and may have different relationships with biometric parameters. Fourth, although we extracted birefringence data of the sclera semi-automatically, the region did not cover the whole anatomical structure of the sclera. For example, the anterior boundary of the region was set at over 10 μm posterior to the tissue surface but not to the boundary between conjunctiva and sclera or Tenon's capsule. This could have reduced the repeatability of the birefringence measurement. Methods of tissue discrimination or boundary detection using PS-OCT could be promising to segment the sclera [60–62]. Usage of these technologies to fully automate the determination of the regions of interest would improve future reliability of the measurements [60–62]. Fifth, the birefringence measured by PS-OCT is affected by the relative angle between a beam and a sample. Although the samples were aligned to be mostly perpendicular to the probe beam, the angle dependence of birefringence might increase a variance of measured birefringence. Sixth, the IOP measured by tonometry might be influenced by corneal elasticity [63]. Although a relationship between corneal elasticity and scleral elasticity has not been investigated, they may be correlated because of their continuous structure with rich collagen fibers. If this assumption is true, the correlation between the measured IOP and the birefringence would be positively biased. However, our results showed a negative correlation, suggesting that the negative correlation found in this study is not an artifact. To exclude the potential influence of the corneal elasticity and to obtain more accurate results, measurement of true IOP is desirable. Seventh, diurnal alteration, reproducibility, and long-term record of IOP were not taken into account in this study.

In summary, scleral birefringence of healthy human eyes was found to be correlated with IOP. Although this finding may indicate that the ultrastructure of collagen fibers in the sclera of healthy eyes is likely to be affected by IOP even in normal ranges as a long-term effect, further studies are required to validate the hypothesis. This study is the first to demonstrate the relationship between scleral birefringence and biometric parameters *in vivo*.

Acknowledgments

This study was supported in part by the Japan Science and Technology Agency under a program of development of systems and technology for advanced measurement and analysis and by Tomey Corporation.

#204494 - $15.00 USD Received 13 Jan 2014; revised 26 Mar 2014; accepted 31 Mar 2014; published 3 Apr 2014
(C) 2014 OSA